ARID ZONE JOURNAL OF ENGINEERING, TECHNOLOGY & ENVIRONMENT
AZOJETE June 2025. Vol.21(2):670-681
Published by the Faculty of Engineering, University of Maiduguri, Maiduguri, Nigeria.
Print ISSN: 1596-2490, Electronic ISSN: 2545-5818
https://doi.org/10.63958/AZOJETE/2025/21/02/030
www.azojete.com.ng

ORIGINAL RESEARCH ARTICLE

INTEGRATING BANDS ALGORITHM ESTIMATION ON WATER TURBIDITY VARIATION IN HARTBEESPOORT DAM, SOUTH AFRICA

G. U. Fayomi [1,2*], E. K. Onyari[2], G.O. Ode[1], and O. I. Nkwonta[3]

[1] *College of Environmental Sciences, Bells University of Technology, Ota, Nigeria*
[2] *Department of Civil and Environmental Engineering & Building Science, University of South Africa, Florida Science Campus, Cnr Christian de Wet Road and Pioneer Avenue, Johannesburg, South Africa*
[3]*Department of Civil Engineering and Surveying Development, Mangosuthu University of Technology, Durban, South Africa*
**Corresponding author's email: fayomiuche@gmail.com*

ARTICLE INFORMATION

Received: 31st August 2024
Revised: 2nd April 2025
Accepted: 3rd April 2025

Keywords:
Remote sensing
Turbidity
Salinity
Landsat 8-9
NDTI
NDSI

ABSTRACT

Water resources remain the most essential need for both human and ecosystems sustenance. Continuous check of both surface and ground water quality remains a welcome approach globally to secure water safety and fitness for different purposes. This study aims to examine the effect of turbidity concentration on water quality of Hartbeespoort dam using remote sensing and Arc GIS. Study objectives examined the present situation of the dam water, access complete one year (2023) data of the water quality variations as weather changes. Remote sensing and Arc GIS application was utilized for this study with the use of Landsat 8-9 Operational Land Imager (OLI) and Thermal Infrared Sensor (TIR). NSMI mapping of turbidity showed high values range of 2.054 high concentration in the month of October, in February, 6.171 in June and 8.273 in October, 2023. NDTI (Normalized Difference Turbidity Index) mapping equally recorded high value of 2.194 in the month of October. The regression analysis utilizes Linear, Exponential and polynomial equation to examine seasonal variation of turbidity in Dam water. The result revealed a strong correlation such as (NDTI in Linear regression analysis records (R^2)= 0.54 while NSMI in linear regression records (R^2)= 0.35. The value derived from NDTI and NSMI algorithm confirmed the capacity of band combination indices in retrieving suspended sediment in form of turbidity using Landsat 8-9. These study findings also punctuate the effectiveness of Landsat8-9 satellite imagery in evaluating turbidity concentration especially in situations where in-situ data is not available.

1.0 Introduction

The usefulness of water quality to human well-being and ecosystem at large escalated the constant demand for continuous monitoring of water safety. Surface water body with measured high-quality content remains very essential for domestic purpose and other uses (Josefin et al., 2022; Seleemi et al., 2022. Water is life and it also serve as a necessary component useful for existence (Zhou *et al.,* 2022). Globally, water issues have been established with simulation of devalued water resource quality having repeated impact on the different uses applicable (Luis *et al.,* 2018). Xiayon & Wu, (2019) reaffirms that water quality reduction is regarded a serious environmental problem that will require efficient water guide and management. This is needed to protect life duration, aquatic survival and biodiversity. There are range of sequential connection relating water quality impact on human health (Omole *et al.*, 2015; Obiloni *et al.,* 2013). The correlation includes water health diseases in form of water borne infections caused by vector carriers and water scarce diseases resulting from water scarcity (Sudheer *et al.,* 2016).

The threat of water quality tends to rise as the population of people increases with inclusion of improved modern technology (Desai and Smt, 2014). Constant water quality check is needed to examine water condition and to establish the fitness for different purposes (Nayla, 2020). It is also necessary to control and prevent

pollution sources to the water body (Issam *et al*., 2023). Water quality indicator is assessed using physical, chemical and biological characteristics. The physio-chemical parameters comprise of total dissolve solid, total suspended solid, pH, dissolved oxygen, chlorine and sodium, turbidity, salinity, chlorophyll and hardness (Issam *et al.,* 2023; Mfesan, 2021). These components generated from series of reactions of the earth natural resources such as the atmosphere, soil, and the water bodies (Xiaoliang *et al.,* 2016; Norman et al., 2020). Josefin *et al.,* (2022) pointed that the connection that exist among the organisms in the earth biotic system such that the damage on one ecosystem affect the others negatively (Takeshi, 2007). Raj *et al.,* (2024) pointed that high turbidity in water body is usually a sign of declined water quality and improper land use. Devendra *et al.,* (2014) pointed that turbidity estimates water muddiness and cloudiness. However, water clearness is known as the brightness and the ability for light to penetrate the water (Adler 2002). The discharge of suspended solid in form of industrial waste discharge, sewage plants domestic wastewater, soil erosion among others exhibits high content of pollutant resulting to water turbidity (Apriwida *et al.,* 2016).

The application of remote sensing and GIS solves the challenge of time consumption, cost and elaborate labour involved in assessing data from larger water bodies. Remote sensing allows summary view of a whole area and ensures broad report of water quality (Mohinuddin *et al.,* 2023; Alice *et al,* 2023; Japitana and Burce, 2019) The findings of the band algorithms and band combination for water quality parameter measurements, establishes that satellite imagery and remote sensing tools is capable and detailed enough for water quality assessment and monitoring (Jing *et al.,* 2020; Yashon *et al*., 2020). Apriwadi et al., (2016) pointed that a considerable measure of turbidity was obtained using band combination of Landsat-5 TM Satellite Image. Tanya and Nicholson (2018) equally confirmed that water quality parameter was derived in Olushange dam with the use of Landsat band 2, band 3, band 4 and band 5. The water quality parameter retrieved include turbidity, total suspended solid, total nitrogen, total phosphorous and algae count. Therefore, this research examined the concentration of turbidity in Hartbeespoort dam utilizing remote sensing and GIS applications. The objectives focused on establishing the current condition of the dam water, acquire complete one-year data of water quality variations and compare the consistence of this study with previous assertions on the water quality of Hartbeespoort dam.

2. Materials and Method

This research methodology involved the adoption of Landsat 8-9 spectral imagery bands featuring double sensors (OLI, TIRS) that operate simultaneously on board (Kristi, 2022). Landsat 8-9 imagery was provided by United States Geological Survey website downloaded from earthexplorer.usgs.gov (NASA/USGS) (USGS, 2020). These two sensors are fully equipped with enhanced adjusted surface reflectance and surface brightness that provides periodic coverage of land features and land mass (Evans *et al.,* (2019); Badawi *et al.,* (2019). Hartbeespoort Dam was obtained from google earth download. Google Earth pro features Google's trademarked software that renders a geographical visual image of earth planet (Cartong, (2021); Tanya & Andrew, 2018) ;). The images were acquired within a period of one year at monthly interval using Landsat 8-9 images which also featured 11 spectral bands of 30meter spatial resolution for bands 1-7 and 15-meters for panchromatic band 8 and band 9-11 (Haobin et al., 2022). Table 2 revealed the features of Landsat 8-9 imagery The detailed of Landsat 8-9 data set imagery and the date it was acquired is shown in table 1. The images were downloaded using Roll 078 and Path 171 that covered Hartbeespoort dam location.

2.1 Study Area

Hartbeespoort dam is the receiving end of Crocodile River basin and Megalies. The dam exhibits a tropical climate like other region with two major seasons which is dry season known as the winter and the summer season which is the rainfall season. The dam is situated Northwest of South Africa between a well-known valley Megaliesberg and Witwaterberg Mountainv 25km away from Pretoria west. Since inception, the dam is known for its declined water quality (Khalid *et al.,* 2022), resulting from major inflow from the Crocodile River with records of high concentrations of phosphates and nitrates (Noloyiso & Silberbauer, 2014). There is also high level of eutrophication recorded issues of the dam due to harmful algal bloom growth. Khalid *et al.,* (2022) identified the major source of pollution to be out flowing waste from industrial processes and domestic effluent. There are several drainage channels connected to the dam. Most of this drainage are discharge flow from wastewater treatment plant, sewage workflow and industrial discharges (Matodzi *et al.,* 2017). Figure 1 shows the location of Hartbeespoort Dam with the different drainage flow that constantly impart the water quality balance in the dam.

Corresponding author's email address: fayomiuche@gmail.com

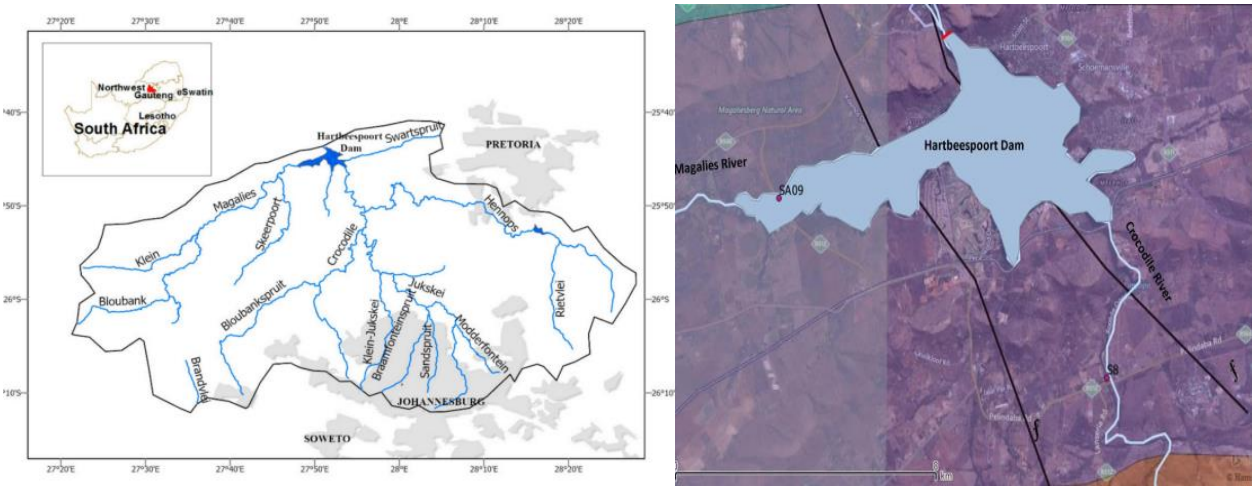

Figure 1: Hartbeespoort Dam location Source and the connecting rivers (Khalid *et al.,* 2022; Matodzi *et al.,* 2017)

Table 1: The dates and other features of Landsat 8-9 imagery acquired (USGS, 2020)

Months	Date Acquired	Land Cloud cover	Ground Control Point Model	Atmospheric Condition
January	1/24/2023	1.77	662	clear cloud condition
February	2/25/2023	0.28	680	clear cloud condition
March	3/29/2023	7.12	548	partly cloudy condition
April	4/30/2023	0.41	648	clear cloud condition
May	5/24/2023	21.81	499	cloudy condition
June	6/25/2023	0.05	660	clear cloud condition
July	7/27/2023	0.52	670	clear cloud condition
August	8/28/2023	0.03	678	clear cloud condition
September	9/5/2023	0.01	663	clear cloud condition
October	10/23/2023	3.31	476	partly cloudy condition
November	11/8/2023	0.04	650	clear cloud condition
December	12/2/2023	0.01	739	clear cloud condition

Table 2: Landsat 8-9 multi spectral bands and its features (Source: USGS, 2022)

Bands	Description	Wavelength (um)	Spatial Resolution (m)
Band 1	Coastal aerosol	0.43-0.45	30
Band 2	Blue	0.45-0.51	30
Band 3	Green	0.53- 0.59	30
Band 4	Red	0.64- 0.67	30
Band 5	Near Infrared (NIR)	0.85-0.88	30
Band 6	Short Wavelengths 1 Infrared (SWIR)	1.57-1.67	30
Band 7	Short Wavelength 2 Infrared (SWIR)	2.11-2.29	30
Band 8	Cirrus (in OLI band 9)	1.36-1.38	15
Band 9	OA bands (available with collection 1)	NA	30
TIRS BANDS			
Band 10	TIRS 1	10.60-11.19	100
Band 11	TIR 2	11.50-12.51	100

2.2 Data Processing Method

Pre-processing improves the quality of the images by reducing the errors connected with data acquisition which can be in form of atmospheric disturbances, topographic constraints, obscurities, and cloud cover properties (Ali *et al.,* 2020). Data processing in this study involves changing of the digital number value to a reflectance value (Adawiah *et al.,* 2021). The Landsat data obtained in raw form must have been affected with atmospheric particles therefore, there is need for the raw number to be corrected into a reflectance value. The processing involves two stages, which include the geometric correction and atmospheric correction DN values" conversion to reflectance values was achieved using raster calculation tool in Arc GIS with the application of equation 1 and 2. (Ali *et al.,* 2020). The formular used for DN value conversion follows:

$$p\lambda = MP\ x\ Qcal + AP \quad 1$$

where: pλ': top-planetary spectral reflectance, lacking solar angle correction, MP: reflectance multiplicative rescaling factor (REFLECTANCE _MULT_BAND_ x, where x is the band number) = 2.0000e-05 available in

Corresponding author's email address: fayomiuche@gmail.com

Landsat8 &9 Meta data file, AP: reflectance additive rescaling factor from the (REFLECTANCE _ADD_BAND_ x, where x is the band number) = − 0.1, Qcal: calibrated standard pixel values (DN)

Solar elevation angle correction equally stands as an important factor to calculate TOA reflectance correction therefore. equation 2 was employed in calculating the sun angle.

$$P\lambda = \rho\lambda\,(sin\,\theta) \quad 2$$

where: Pλ = top-of-atmosphere planetary reflectance, θ = sun elevation angle (from the Meta data file of the OLI raw data

2.3 Employed Algorithm

The Normalized Difference Turbidity Index (NDTI) utilized in this study is a constant valued tool for assessing the changes in water quality, confirming water pollution levels, and aiding in the efficient control of freshwater resources. This index employed the modality measurements acquired with the use of remote sensing equipped tools to determine water turbidity (Raj, *et al*., 2024). The sequence analysis focused on band combination index after atmospheric corrections (Haobin et al., 2022). The NDTI index utilized two major spectral bands which is the red and green band sensitive to suspended solid particles and turbidity. The values of NDTI range from − 1 to 1. The positive values show higher turbidity, while negative values indicate low turbidity (Garg et al., 2020; Raj *et al*., 2024). Equation 3 revealed NDTI indices

$$NDTI = \frac{Red-Green}{Red+Green} \quad 3$$

$$NDTI = \frac{Band\ 4 - Band\ 3}{Band\ 4 + Band\ 3} \quad 4$$

2.4 Normalized Suspended Material Index (NSMI)

NSMI index is also an essential algorithm for retrieval of suspended material that mostly affect water turbidity. NSMI was equally employed to further confirm the concentration of turbidity. It was established following the ideologies that clear water possesses highest reflectance in the blue band while the existence of suspended material promotes an increase of reflectance in the visible range band of green and red (ρ red + ρ green) where clear water inclines to grip radiation (Fatemeh *et al.,* 2021. The formular for NSMI is shown in equation 5 & 6. All the bands value used in this algorithm were adjusted to a reflectance value.

$$\text{NSMI} = \frac{Red\ band + \text{Green}\ band - Blue\ band}{Red\ band + Green\ band + Blue\ band} \quad 5$$

$$\text{NSMI} = \frac{Band4 + \text{Band3} - Band2}{Band4 + Band3 + Band\ 2} \quad 6$$

2.5 Modified Normalized Difference Water Index (MNDWI)

Separating Water-only image from vegetation was achieved with the use of the Modified Normalized Difference Water Index which enhances the water with the use of Green and SWIR band (MNDWI) (Xu, 2006). This was also supported with clipping data management in Arc GIS and digitizing of the water area out from google earth as shown in Plate (1a) & (1b). MNDWI formular is shown in equation 7.

$$\text{MNDWI} = \frac{(P_{green} - P_{MIR})}{(P_{green} - P_{MIR})} \quad 7$$

$$\text{MNDWI} = \frac{(\text{Band3} - \text{Band6})}{(\text{Band3} - \text{Band6})} \quad 8$$

Corresponding author's email address: fayomiuche@gmail.com

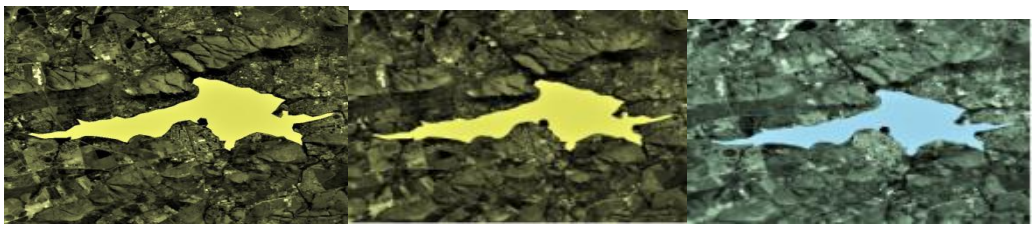

Plate 1a: Showing the band imagery and clipped water location.

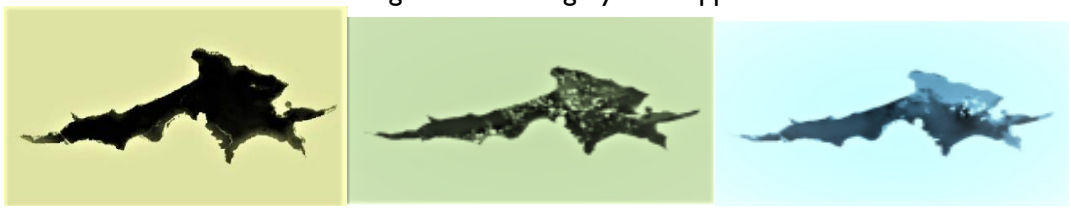

Plate 1b: Shows the process of separating only water image.

3. Results and Discussion

The result derived from the analysis validates the capacity of each algorithm employed in mapping out turbidity concentration in the Dam water as revealed in Table 3 which is the variations of turbidity concentration in the Dam. The Normalized Difference Turbidity Index (NDTI) in Landsat 8-9 were projected by applying the spectral reflectance of green band with wavelength of (0.53- 0.59) and red band with wavelength of (0.64-0.67) with same 30m spatial resolution estimated the turbidity of water bodies due to their spatial reflectance to light. This allows easy penetration of the spectral bands into the water features (Khan *et al.,* 2001). NSMI index in Landsat also utilized same spectral band green, red and blue with wavelength of (0.45-0.51) essential algorithm normally used for retrieval of suspended material that normally affect water turbidity. In Figure 2, the NDTI and NSMI was calculated for each month using the acquired Landsat data after atmospheric correction. The value derived was checked with each month to examine turbidity variations affecting water quality. The equation coefficients that have the highest correlation (R^2) value was also regarded suitable for turbidity concentration estimation in surface water body. The value of NTDI and NSMI index algorithm with a positive value denotes turbid water and a higher concentration of suspended particles, while a negative value denotes clear water and a low degree of turbidity.

Table 3: Positive turbidity value from Indices Employed

Months Variations	NDTI (B4, B3)	NSMI (B4, B3, B2)
January (1)	0.034	0.180
February (2)	0.418	2.054
March (3)	0.436	1.155
April (4)	0.409	1.670
May (5)	0.417	1.407
June (6)	0.416	6,171
July (7)	0.120	0. 506
August (8)	0.411	0.519
September (9)	0.419	0.528
October (10)	2.194	8.273
November (11)	0.418	0.516
December (12)	-0.406	0.473

The regression analyses carried out between the two indices exposed strong positive relationships with some of the equation model. Several studies from literatures have established the potentials of remote sensing application and the utilization of band combination indices in observing water quality changes (Raj et al.,2024, Aditya, 2019, Adel et al., 2023). Three different regression patterns shown in Figure 3 was employed to check variation analysis of turbidity concentration using NDTI and NSMI. Landsat value in Linear regression equation in NDTI acquired the highest reflectance value of (R^2) value = 0. 54 while Polynomial and Exponential equation recorded a lower value of (R^2) value = 0.13 respectively. This confirmed the capacity of linear regression equation having the potency to deliver precise estimation of turbidity concentration in both lower and high turbid water because it has proven to obtain best value. However, the results obtained from NDTI was confirmed further by utilizing NSMI with the three-regression equation.

Corresponding author's email address: fayomiuche@gmail.com

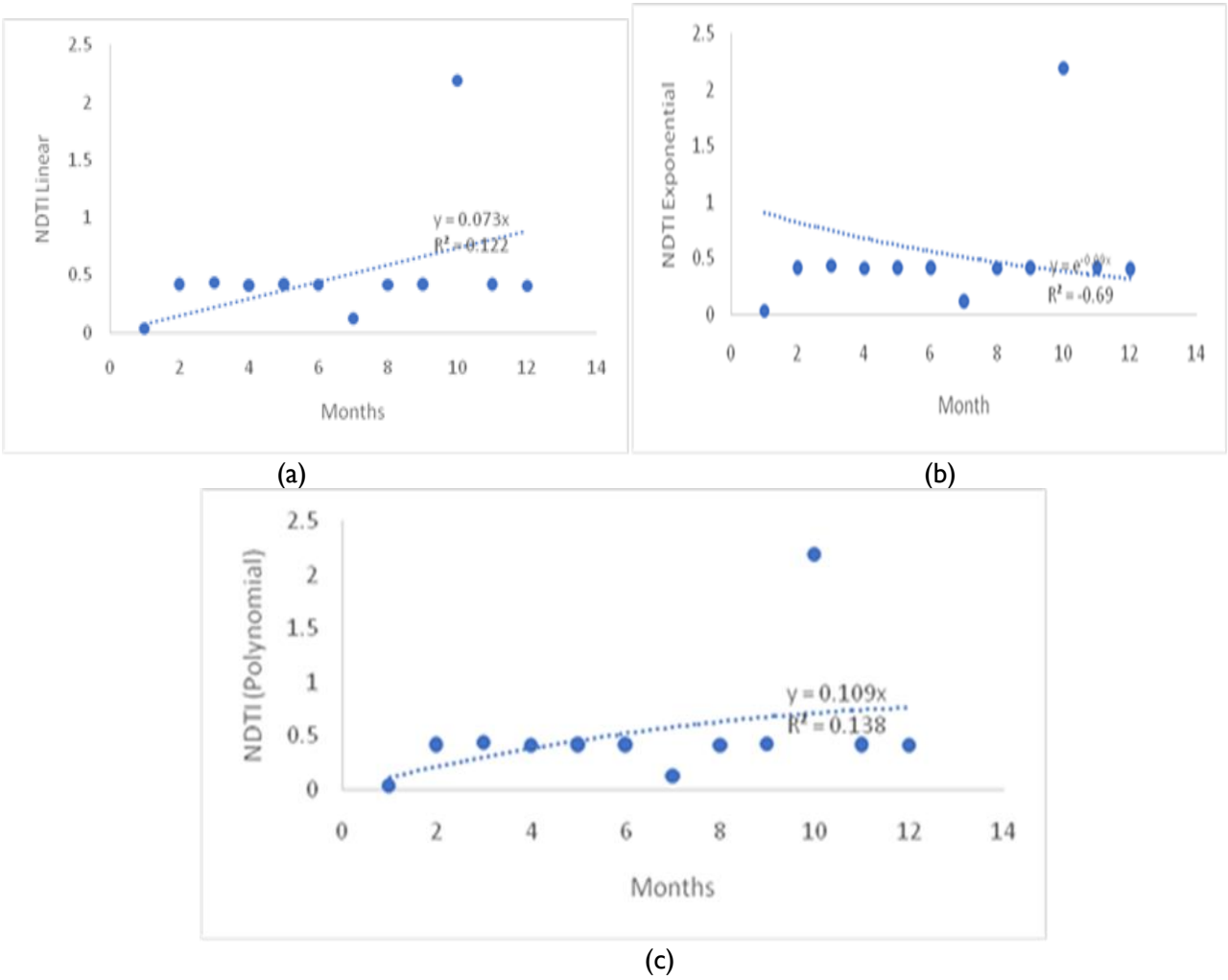

Figure 2: The NDTI variation measurement on a) Linear, b) Exponential, and c) Polynomial regression.

Figure 3 revealed the result from the regression analysis. linear equation recorded the highest correlation coefficient of (R^2) = 0.35 and other equation recorded very lower reflectance value and therefore, regarded not fit for turbidity estimation. The result generated using NDTI in Landsat 8-9 shows the efficiency of the spectral sensors band value and Linear regression equation having expressed a better potential in estimating turbidity concentration.

3.1 Turbidity Variations and Mapping

Turbidity measures the volume of suspended solid particles in the water and remains as one of the optical water features that disperse light instead of gripping light. The dispersing of the light is due to the presence of suspended substances in the waterbed (Gholizadeh *et al*., 2016). Turbidity is measured in NTU it can range from less than 10 Nephelometric turbidity units (NTU), which indicate a very clear water to over 1000 NTU (very muddy or not clear) (Mike 2009). The result derived from NDTI mapping in Hartbeespoort Dam varies from 0.120 to 2.194 high turbid concentration measures. Figure 4 shows the map variation of NDTI turbidity on monthly basis. From the analysis, the dam featured more on very low turbidity concentration characterizing water clarity with less suspended solid in this period. NDTI mapping only records the highest value in the month of October with value ranging from – 2.194. Other months recorded higher value concentration of 0.411-0.406 apart from the months January with records of 0.034 and 0.120 in July, 2024. The period of heavy flow that is the Autumn season between March to June (Conerlius *et al*., 2018). This period is meant to have high turbidity concentration base on the assertion made by (Matodzi et al., 2017). These changes might be due to weather changes, climate factors or lesser activities during this period

Corresponding author's email address: fayomiuche@gmail.com

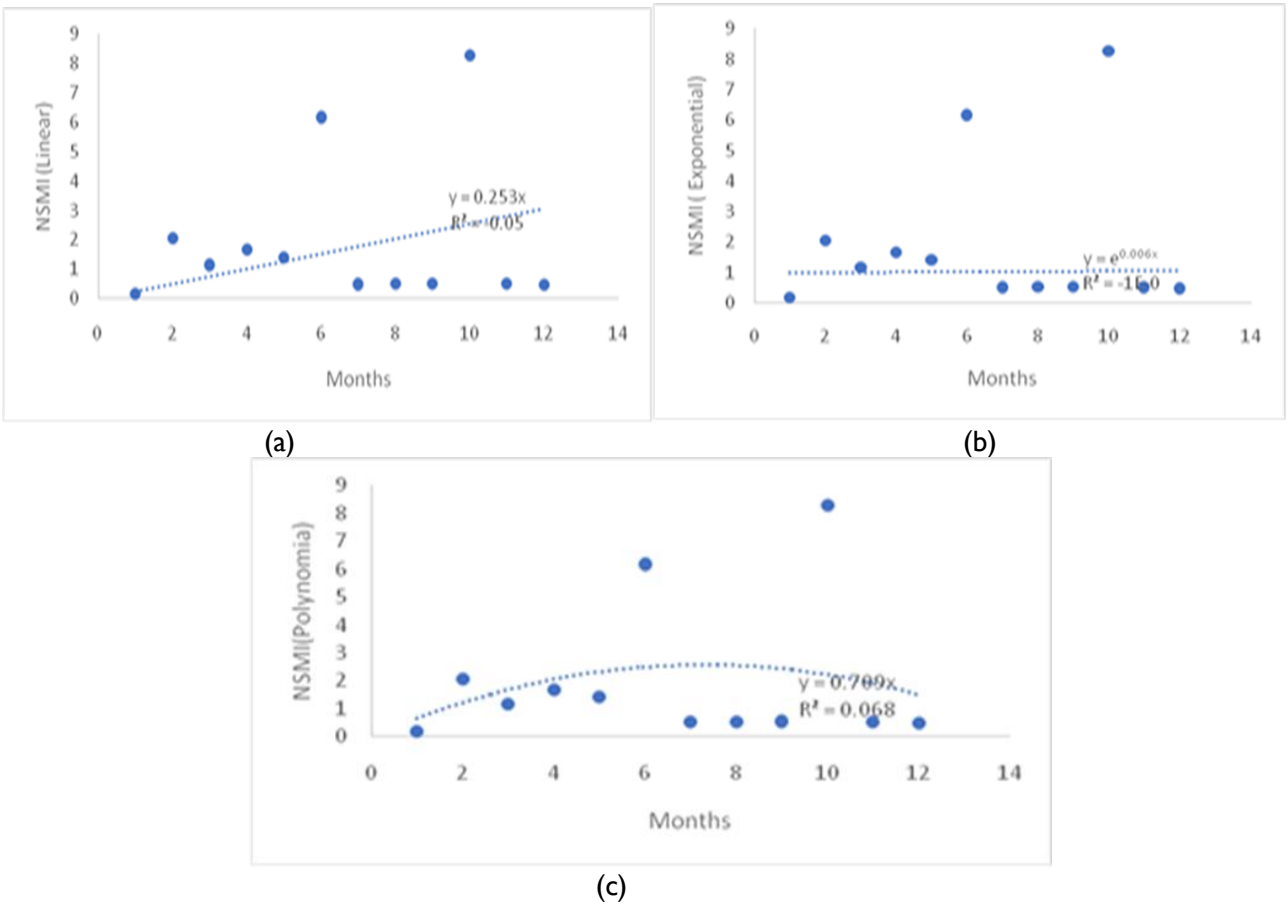

Figure 3: The NSMI variation measurement on a) Linear, b) Exponential, and c) Polynomial pattern.

3.2 Turbidity Variations and Mapping

Turbidity measures the volume of suspended solid particles in the water and remains as one of the optical water features that disperse light instead of gripping light. The dispersing of the light is due to the presence of suspended substances in the waterbed (Gholizadeh *et al.*, 2016). Turbidity is measured in NTU it can range from less than 10 Nephelometric turbidity units (NTU), which indicate a very clear water to over 1000 NTU (very muddy or not clear) (Mike 2009). The result derived from NDTI mapping in Hartbeespoort Dam varies from 0.120 to 2.194 high turbid concentration measures. Figure 4 shows the map variation of NDTI turbidity on monthly basis. From the analysis, the dam featured more on very low turbidity concentration characterizing water clarity with less suspended solid in this period. NDTI mapping only records the highest value in the month of October with value ranging from – 2.194. Other months recorded higher value concentration of 0.411-0.406 apart from the months January with records of 0.034 and 0.120 in July, 2024. The period of heavy flow that is the Autumn season between March to June (Conerlius *et al.*, 2018). This period is meant to have high turbidity concentration base on the assertion made by (Matodzi *et al.*, 2017). These changes might be due to weather changes, climate factors or lesser activities during this period.

In this study, mapping of high turbid region using NSMI value varies in the different months. The value ranges from 0.155 being the lowest to 8.273 as the highest. Although, NSMI value in Figure 5 & 6 recorded maximum higher value than NDTI with very huge different in some months. For instance, in the month of February, NSMI image of Landsat 8-9 (OLI & TIR) revealed the concentration of turbidity in Hartbeespoort Dam water within the range of -0.506 to 2.054, the higher concentration in the month of February displays dark blue colour and in the month of June NSMI have value range of -23.768 to 6.171 high with display of yellow colour. Also, in the month of October records ranges from – 9.690- 8.273 high with display of dark blue colour. However, the area with lower concentration or clear water area also recorded higher value than the area with high turbid concentration. The general result is showing moderately high and low turbidity variation in fresh dam water according to freshwater turbidity standard (Conerlius *et al.*, 2018). This situation could be ascribed to seasonal changes in rainfall pattern and temperature. Figure 7 shows the rainfall data with high precipitation from the month of February, March, April, May and November, 2023 validating the reason for moderately high turbidity mapping during this time.

Corresponding author's email address: fayomiuche@gmail.com

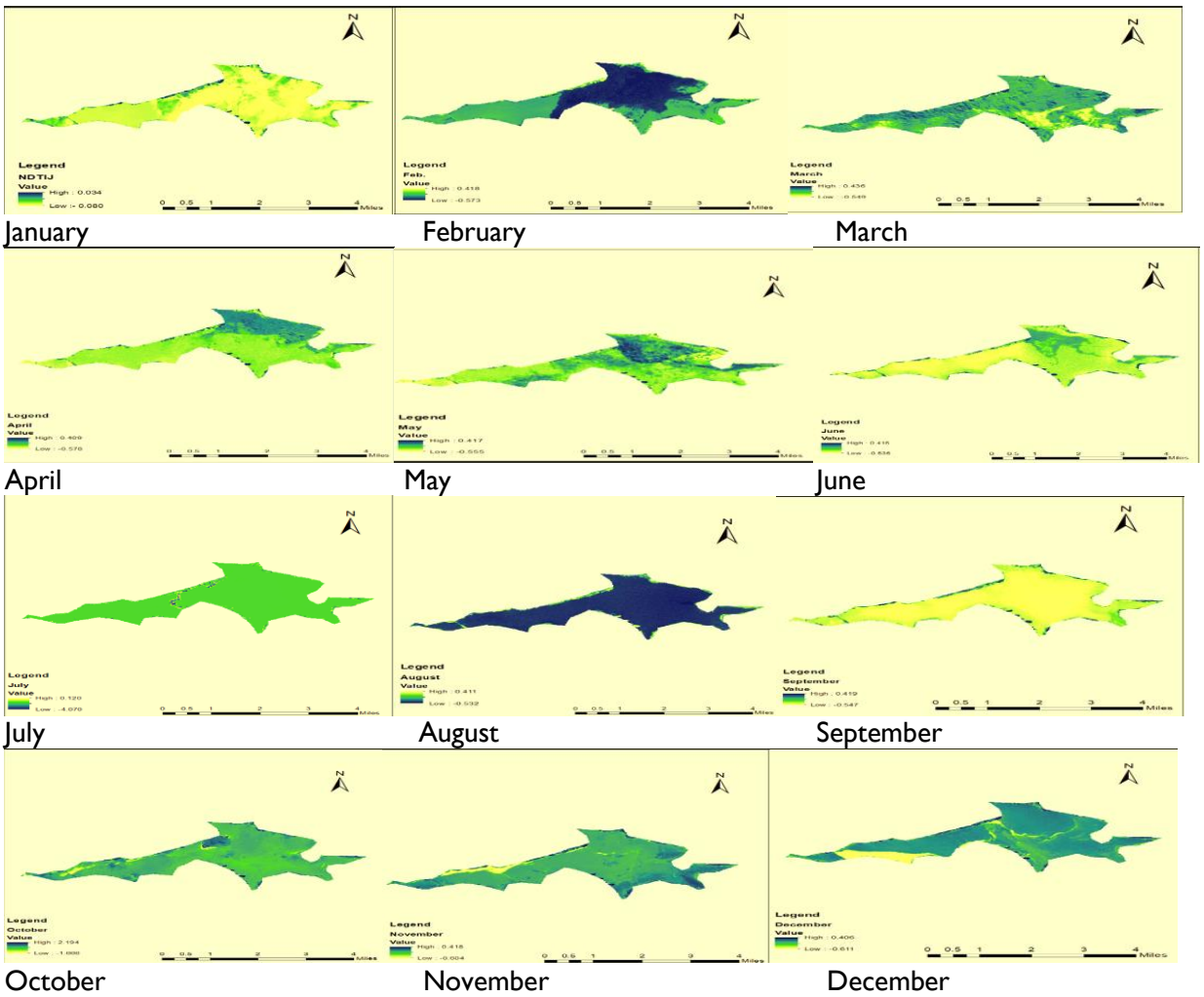

Figure 4: NDTI Mapping

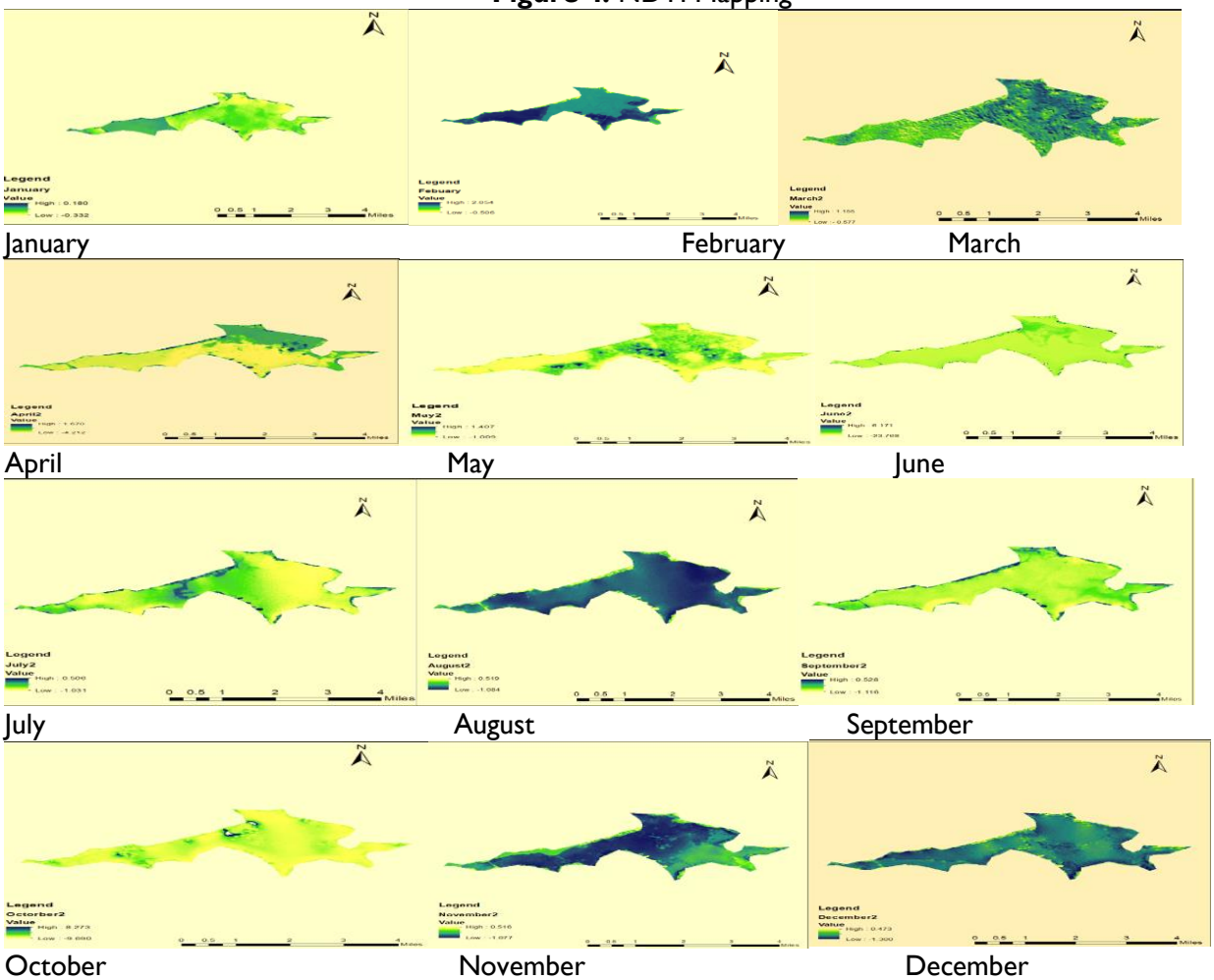

Figure 5: NSMI Mapping

Corresponding author's email address: fayomiuche@gmail.com

However, Low precipitation was noted in Jan, and picks up again from June- Nov 2023 which was the reason for lower mapping. Similarly, urban activities around the area could also be a major factor as it was confirmed that the dam water is a pick-up point of particles and pollutant from the connecting rivers and wastewater plants, agricultural and industrial processes (Khalid et al., 2022). Figure 6 shows the performance of the two indices applied

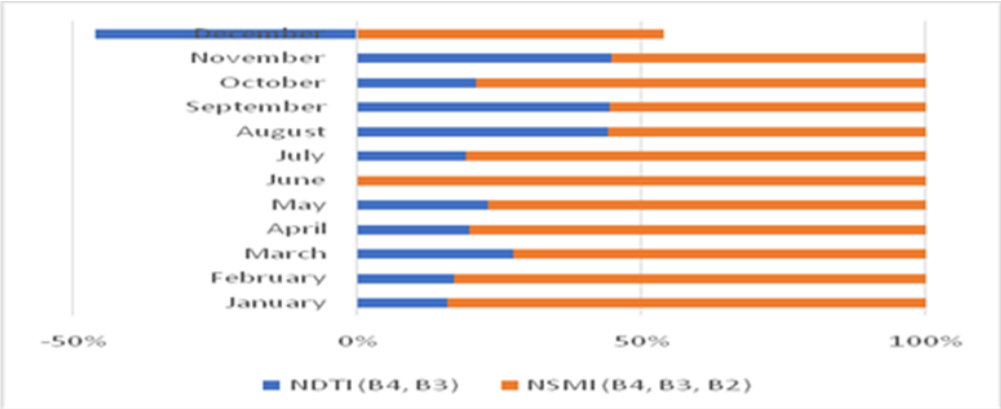

Figure 6: NSMI and NDTI Rating

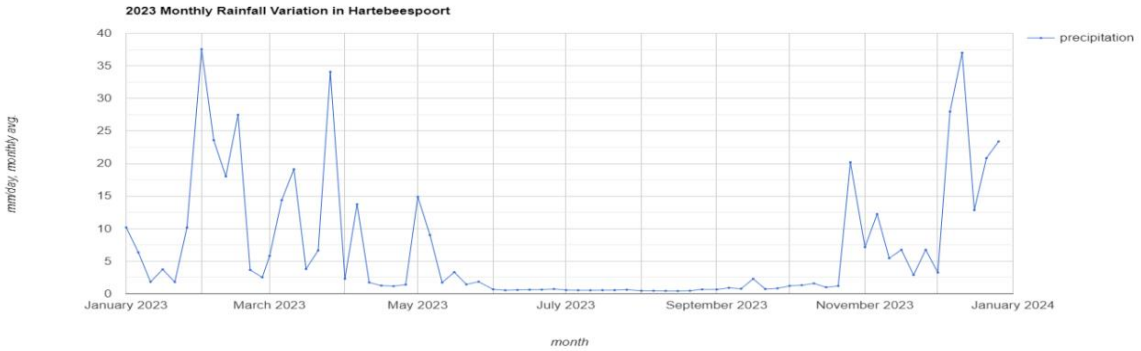

Figure 7: Rainfall data in Hartbeespoort location for the study period

4. Conclusion

The study evaluated the performance NDTI and NSMI in mapping out turbidity concentration in Hartbeespoort Dam. However, evaluating turbidity levels in dam water is vital for conserving water usefulness, fitness and functionality. The study investigated and mapped the distribution of turbid water using multi-spectral resolution spatial bands of Landsat 8-9 (OLI & TIR). The bands involved Band 3 (green) Band 4 (red) and Band 2(blue) used in both NDTI and NSMI. The relationship among the results of NDTI and NSMI was correlated with the different months to examine the variation impact of turbidity as weather changes and to also understand the potentials of using band combination indices to evaluate turbidity. Linear regression equation coefficient recorded the highest reflectance value of (R^2) = 0.53 in NDTI and (R^2) = 0.35 in NSMI. Although, utilization of all the index algorithm in evaluating turbidity concentration in dam water indicated the presence of significant volume of turbidity which usually result to aesthetic problem and general water decline of the dam. The contributing factor could be traced to implication of urban runoff from the surrounding land activities that is majorly agricultural farms around the dam and other climate factors. However, the connecting river such as Jukskei and Crocodile constantly flush in dark water and increasing the concentration of sediments in the water. The study demonstrated the usefulness of engaging satellites acquired data of Landsat 8-9 equipped sensors spectral band combination to monitor turbidity concentration in freshwater dam. The study has also generated significant result that will serve as a guide for resource managers and policymakers to watch out for water quality seasonal variations and also target a rectification effort. NDTI and NSMI performed better in mapping out turbidity with little variations in some period. Therefore, it is thus recommended that further research can be conducted for confirmation of the utilized algorithms in the same location and the developed model potency for water quality assessment.

Corresponding author's email address: fayomiuche@gmail.com

References

Aditya Sandeep K. 2019. Estimation and mapping of Turbidity in the lower Charlse River using Landsat 8 OLI Satellite Imagery, Theses.

Adawiah SW., Setiawan KT., Parwati E. and Faristyawan, R. 2021. Development of empirical model of Total Suspended Solid (TSS) by using Landsat 8 on the Coast of Bekasi Regency. Earth and Environmental Science 750, 012039.

Adel JA., Mutasim Ibrahim Malik, MI. and Abduljabbar, HM. 2023. Utilizing Spectral Indices to Estimate Total Dissolved Solids in Water Body Northwest Arabian Gulf. Indonesian Journal of Marine Sciences September, 28(3):217-224.

Alice, NO., Yashon, O., Kosgeia, JR., Kongob, V., Kemboia, EJ., Simon, MNSM., Achisa, CMA. and Kipkorira, EC. 2023. Estimation and mapping of water quality parameters using satellite images: a case study of Two Rivers Dam, Kenya, Water Practice & Technology, 18 (2): 428. Doi: 10.2166/wpt.2023.010.

Ali AA. M., Ali C, Maitham AS., Hashim, BM., Hussain MH. and Nadhir Al-Ansari, N. 2020. Estimation of Total Dissolved Solids in water bodies by spectral indices Case study: Shatt al-Arab River Water Air Soil Pollut. 231: 482 https://doi.org/10.3390/rs14174277.

Adler, JH 2002. Fables of the Cuyahoga Reconstructing. A History of Environmental Protection Fordham Environmental law journal, 14: 89-146.

Apriwida Y., Bowo S. and Pramaditya W. 2016. The application of Landsat 8 OLI for Total Suspended Solid (TSS) mapping in Gajahmungkur Reservoir Wonogiri Regency. Conf. Series: Earth and Environmental Science, 47: 012028

Badawi, MD., Helder, LL. and Jing, XJ. 2019. Methods for earth-observing satellite surface reflectance validation. Remote Sensing, 11(13): 154.

Cartong, E. 2021. Mapping Basics Within Google Earth Pro-Info @ cartong.ORG. www.CARTONG. ORG 2021.

Cornelius R., Odusanya, D., Weiss, JM., Jacob de B. and Chimuka, L. 2018. Seasonal variation of chloro-s-triazines in the Hartbeespoort Dam catchment, South Africa. Science of the Total Environment. 613–614

Desai. N. and Smt, V. 2014. A study on water pollution base on the environmental problem. Indian journal of Research, 3: 395-96.

Devendra D., Shriram D. and Atul K. 2014. Analysis of ground water quality parameters, A review. Research journal of engineering science, 3(5): 26-31https://doi.org/10.4236/oalib.1105785.

Evan, AK., Abghy AP., Ayudyanti, AG., Huda, M., Sabrina, RNF and Anindya, S. 2019. Total Suspended Solid (TSS) estimation in Lake Tempe, South Sulawesi using Sentinel-2B Imagery. Easy Chair Preprint No 1957.

Fatemeh G., Navid, G., Ahad, N. and Timmor, BN. 2021. Monitoring soil salinity changes, comparison of different maps and indices extracted from Landsat satellite images (Case study: Atabieh, Khuzestan) Pol. J. Environ. Stud, 30(2): 1139-1154.

Garg, V., Aggarwal, SP. and Chauhan, P. 2020. Changes in turbidity along Ganga River using Sentinel-2 Satellite Data during lockdown Associated with COVID-19. Geomatics, Nat. Hazards Risk 11(1): 1175–1195. https://doi.org/10.1080/ 19475705.2020.1782482.

Gholizadeh M., Melesse A. and Reddo L. 2016. A comprehensive review on water quality parameter estimation using remote sensing techniques. Sensors 16 (8): 1298.

Haobin M., Jing Z. and Zhen Z. 2022. Retrieving inland reservoir water quality parameters using Landsat 8-9 OLI and Sentinel 1-2 MSI Sensor with Empirical Multiva-riate Regression. Environ. Res. Public health 19: 7725.

Corresponding author's email address: fayomiuche@gmail.com

Issam A. Al-Jabari, A.M. and Al-Oqaili, M. 2023. Assessment of bacteriological quality and physiochemical parameter of domestic water sources in Jenin Governorate. A case study. Journal of Environmental and Public Health, Doi. 10.3390/ijerph7103657.

Japitana MVS., Burce MEC. 2019. A satellite base Remote Sensing Techniques for surface water quality estimation. Engineering technology and applied science research, 9(2): 3963-3370.

Jing Z., Zhang, F., Chen, S., Wang, C., Chen, J., Zhou, H. and Xue, Y. 2020. Remote sensing evaluation of Total Suspended Solids dynamic with Markov Model: A Case study of Inland Reservoir across Administrative Boundary in South China. Sensor**s** (20): 6911 doi:10.3390/s20236911

Josefin TM., Bierkens, FP., Anna Scaini, E., Sutanudjaja, H. and Van Vliet, THM. 2022 Salinity impacts on irrigation water-scarcity in food bowl regions of the US and Australia. Environ. Res. Lett., 17: 084002.

Khalid A., Abiye, T., Adam, E. 2022. Integrating in suit and current generation satellite data for temporal and spatial analysis of harmful algea bloom in the Hartbeespoort Dam, Crocodile River Basin, South Africa. Journal of Remote Sensing, 14(7): 4277-4280 https:// Doi.org/10.3390/rs14174277

Khan, NM., Rostoskuer, VV., Shalina, EE. and. Sato. Y. 2001. Mapping soil affected soil using remote sensing indicators in a simple approach with the use of GIS IDRISI 22nd Asian Conference on Remote Sensing, 5 (9).

Kristi, S. 2022. Landsat 8-9 Collection 2 (2) Level 2 Science Product (L2SP) Guide. Department of the Interior U.S. Geological Survey.

Luis, C., Gonzalez-Marquez, F., M.,Torres, Bejarana AC., Torregraza-Espinosa, I. R., Hansen- Rodriquez, HB. and Rodriques G. 2018. Use of Landsat 8 images for depth and water quality assessment of El Guajoro Reservoir Columbina. Journal of South American Earth Sciences, 82: 231-238.

Matodzi MM., Mmakosha IM. and Murembiwa SM. 2017. The economic effect of Hartbeespoort Dam area. Conference paper.

Mfesan GN. 2021. Application of statistical techniques on the assessment of water quality parameters. Master of science. http://hdl.handle.net/10210/484224.

Mike S. 2009. The basics of turbidity measurement Technologies. Data Comparability Board QA/QC Sensors Group

Mohinuddin, SK Soumita S., Sarkar, B., Ujwal, DS., Aznarul I. A., Islam, RM., Hossain, SZ., Sadik M., Taushik A., Raju Mondal, R., Zhang, W. and Aimun, B. 2023. Assessing Lake water quality during COVID-19 era using geospatial. Techniques and artificial neural network model. Environmental Science and Pollution Research, 30(1): 65848–65864

Nayla OH. 2020. Water quality parameters. Intech open publisher Doi;10.5772/intech open.89657.

Norman EP., Michel M. and Chapman, DV. 2006.effect of human activities on water quality. Net publication/2294528 Doi-10.1002/04708488944/hsa096.

Noloyiso XM. and Silberbauer, M. 2014. Investigating of the effectiveness of techniques deployed in controlling cyanobacterial growth in Rietvien Dam in Crocodile (West) and Marico water Management Area. Degree of Master of Science.

Omole, DO, Emenike, CP., Tenebe, IT., Akinde, AO. and Badejo, AA. 2015. An assessment of water related diseases in a Nigerian community. Research Journal of Applied Sciences, Engineering and Technology 10(7): 776-781.

Obilonu, AN, Chijioke, C., Igwegbe, WE., Ibearugbulem, OI. And Abubakar, YF. 2013. Water quality challenges and impact. International Letters of Natural Sciences, 4, (44- 53).

Corresponding author's email address: fayomiuche@gmail.com

Raj, S., Saritha, V., Chaitanya B. and Pande, CP. 2024. Monitoring of wetland turbidity using multi-temporal Landsat-8 and Landsat-9 satellite imagery in the Bisalpur wetland, Rajasthan, India. Environmental Research 241(1): 117638-117640.

Seleemi TD., Bafi, M., Karantzia, I. and Parchridis, E. 2022. Water quality monitoring using Land Landsat 8 and Sentinel-2 satellite data in Timsah Lake, Ismailia, Suez Canal Regions (Egypt). Journal of Indian Society of Remote Sensing, 50(12): 2411-2428.

Sudheer K., Chaubey I. and Garg V., 2016. Lake water quality assessment from Landsat Thermatic Mapper data using Neural Network: An approach to optimal Band Combination Selection 1. Wiley online Library, New York.

Tanya K. and Nicholson, A. 2018. Using Google Earth Pro University of Toronto Mississauga Library Hazel McCallion Academic Learning Centre, 7(3.2) https://library.utm.utoronto.ca/datagis/statistical.

Takeshi, G. 2007. Monitoring and measuring of water Quality parameter (270-275) https://org/10.1080/0790062880/8722401.

Xiayon, W. and Wu, Y. 2019. Water quality monitoring and evaluation using remote sensing techniques in China: A systematic review. Journal of ecosystem health and sustainability, 3 (5).

Xiaoliang J., Randy A. and Zhang, DM. 2016. Comparison of seven water quality assessment methods for the characterization and management of highly impaired river systems. Environ Monti Assess 188: 15. DOI 10.1007/s10661-015-50162.

Xu H.Q. 2006. Modification of Normalized Difference Water Index (NDWI) to enhance open water features in remotely sensed imagery. Int. J. Remote Sens., 27(14): 3025–3033.

USGS, 2020. Landsat 8-9 Operational Land Imager (OLI) and Thermal Infrared Sensor (TIRS) Collection 2 Level-1 15- to 30-meter multispectral data. Earth Resources Observation and Science (EROS) Center.

Yashon OO., Kimutai N. and Kipkemoi H. 2020. Modelling reservoir chlorophyll-a, TSS, and Turbidity using Sentinel-2A MSI and Landsat-8 OLI satellite sensors with empirical multivariate regression Hindawi Journal of Sensors, 2020(21). https://doi.org/10.1155/2020/8858408.

Zhou, L., Appiah, R., Boadi, EB., Ayamba, EC., Larnyo, E.. Antwi, HA. 2022. The Impact of human activities on river pollution and health-related quality of life: Evidence from Ghana. Sustainability, 14:13120. https://doi.org/10.3390/su142013120.

Corresponding author's email address: fayomiuche@gmail.com